Available online at www.sciencedirect.com
ScienceDirect
Ceramics International 35 (2009) 195–198
CERAMICS INTERNATIONAL
www.elsevier.com/locate/ceramint

Chemical reduction of nanocrystalline CeO_2

Slavica Zec *, Snežana Bošković, Branka Kaluđerović, Žarko Bogdanov, Nada Popović

Institute of Nuclear Sciences Vinča, 11001 Belgrade, POB 522, Serbia

Received 3 September 2007; received in revised form 9 September 2007; accepted 2 October 2007
Available online 25 December 2007

Abstract

The reduction of commercial and mechanochemically processed CeO_2 powders was studied. Nanostructured CeO_2, with the crystallite size of 21 nm and the lattice distortion of 0.37%, was obtained during 60 min of milling in a high-energetic vibratory mill. X-ray diffraction, scanning electron microscopy and Brunauer-Emmett-Teller method were applied to characterize the milled powders. During the thermal treatment at 1200 and 1400 °C in an argon atmosphere the nonstoichiometric CeO_{2-x} oxides with the defect fluorite structure were formed. Compositions of CeO_{2-x} oxides were determined according to its lattice parameter. The results showed that the release of oxygen, as well as the rate of reduction, was more effective in nanocrystalline then in the microcrystalline CeO_2, producing at 1200 °C $CeO_{1.80}$ and $CeO_{1.85}$ oxides, while at 1400 °C were obtained similarly, $CeO_{1.77}$ and $CeO_{1.78,}$ compositions.

Keywords: A. Milling; B. X-ray methods; D. CeO_2; Nanostructure

1. Introduction

Cerium dioxide (ceria, CeO_2) and ceria based materials are promising materials for number of applications, so they have been widely investigated in recent years. Ceria is becoming an important material in various fields of modern technology, such as catalysis, microelectronics, optoelectronics, electrochemical devices, ultraviolet blockers, etc. [1–3]. Its different functions are mainly related to the ceria existence in two oxidation states, trivalent and tetravalent, and the Ce^{4+}– O^{2-} charge transfer. Among the numerous cerium oxides [4], the nonstoichiometric oxides, CeO_{2-x}, which has a defect structure of the same fluorite type as ceria, is extensively studied owing to its redox capability and ionic conductivity [5]. Depending on the temperature and the partial oxygen pressure, CeO_{2-x} exists in the composition range $0 < x < 0.3$ [6,7]. Point defects of CeO_{2-x} structure arise due to the loss of oxygen and formation of oxygen vacancies, as well as due to reduction of Ce^{4+}- into Ce^{3+}-ions in order to charge neutrality preservation.

At present, great attention is paid to production of nanocrytalline CeO_2 powders, expecting better catalytic activity, redox properties and a higher ionic conductivity in comparison to those of the microcrystalline CeO_2. Decreasing of the crystallites size into nanometer range enhances redox capability and ionic conductivity of CeO_2 owing to the higher mobility, primarily of the oxygen ions. Several methods have been developed to synthesize nanosized CeO_2 powders, such as precipitation [8], solid-state reaction [9], mechanochemical processing [10], combustion synthesis [11], self-propagating synthesis [12] and other.

The reduction of mechanochemically produced nanosized CeO_2 powder was studied in this paper while, to the best of our knowledge, the reduction of ceria prepared in this way was not studied before. For the sake of comparison, we have also studied the reduction of commercial microcrystalline CeO_2 powder during thermal treatment in an argon atmosphere.

2. Experimental procedure

Commercial CeO_2 powder (Aldrich, 99.9%, particle size <5 μm) was milled in high-energetic vibratory mill, Pulverisette 9 (Fritsch), with tungsten carbide (WC) lining and grinding media. Ten grams of the oxide powder were milled for 2, 15, 30, 45, 60, 90 and 120 min. Reduction of CeO_2 powders was performed in an Astro furnace in a flowing argon (99.95%,

* Corresponding author. Tel.: +381 11 2439454; fax: +381 11 2439454.
E-mail address: zec@vin.bg.ac.yu (S. Zec).

0272-8842/$34.00
doi:10.1016/j.ceramint.2007.10.031

flow 20 l/h) atmosphere under oxygen partial pressure less than 50.65 Pa. Powders were pressed uniaxialy into pellets (diameter 10 mm, height ~10 mm) in a steel die under 35 MPa. Pellets, put into boron nitride coated graphite vessel, were fired at 1200 and 1400 °C for 1 h. Specimens were furnace cooled under argon to room temperature. Starting and milled CeO_2 powders were characterized by X-ray powder diffraction analysis (XRD), scanning electron microscopy (SEM) and specific surface area obtained by Brunauer-Emmett-Teller (BET) method, while the powders of the fired samples were examined by XRD.

SEM was performed by JEOL JSM-35 equipment. The specific surface area was calculated from N_2 adsorption measured at 77 K.

2.1. XRD characterization

XRD analysis was carried out by a Siemens D500 diffractometer in the range from 20 to 80° 2θ using Ni-filtered Cu Kα radiation and the scanning speed of 0.02° (2θ)/s, while the data were processed by Diffrac^{plus} software. Phases were identified according to the ICDD-PDF data base [13]. Owing to the different mass absorption coefficients (μ_m) of CeO_2 (333.7 cm^2/g) and WC (160.8 cm^2/g) for CuKα radiation, quantity of WC, introduced in the system during milling, was determined from the integral intensity relation (I/I_0) of the WC 1 0 0 peak using expression for the two-component mixture [14]:

$$\frac{I_1}{(I_1)_0} = \frac{w_1\mu_{m1}}{w_1(\mu_{m1} - \mu_{m2}) + \mu_{m2}}$$

in which w is weight fraction of the components, while I and I_0 are intensities of the component's convenient peak in the mixture and the same peak of the pure component, respectively.

The average crystallite size and mean lattice distortion of CeO_2 were obtained on the basis of the full width at half maximum intensity (FWHM) of the 1 1 1, 2 0 0, 2 2 0 and 3 1 1 peaks of CeO_2, measured after the separation of the Kα-doublet by Diffrac^{plus} software. Calculation of the crystallite size and lattice distortion was performed applying Williamson-Hall method and Cauchy expression [15]:

$$\beta\cos\theta = \frac{K\cdot\lambda}{D} + 4\cdot\varepsilon\sin\theta$$

in which the total peak broadening (β) is the sum of peak broadening due to crystallite size (D) and broadening due to lattice distortion (ε). Elimination of the instrumental broadening was done using an empirical formula: $\beta = B - b^2/B$, where B represents the measured peak width, while b is the instrumental width obtained from a Si standard.

Lattice parameter of the cerium oxides with the fluorite structure was refined by the WINCELL program. Compositions of the nonstoichiometric CeO_{2-x} oxides formed in the fired samples were calculated from Kim's empirical relation expressed as [16]:

$$a = 5.413 + 0.4612x\,(\text{Å})$$

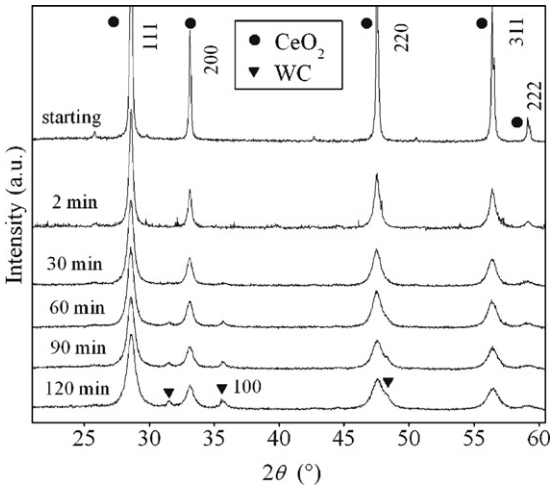

Fig. 1. XRD patterns of CeO_2 powders milled for various time.

which gives dependence between the lattice parameter a of CeO_{2-x} and x in CeO_{2-x}.

3. Results and discussion

XRD patterns of the starting and milled CeO_2 powders (Fig. 1) reveal the broadening of CeO_2 reflections as the milling time got longer and the appearance of WC reflections after 30 min of milling. The CeO_2 starting powder had the crystallite size of 140 nm and no significant lattice distortions, while its lattice parameter $a = 5.412(1)$ Å was not changed during milling.

In the first 30 min of milling (Fig. 2), a rapid decrease of CeO_2 crystallite size occurred while its lattice distortion attained maximum. A steady state was already achieved in the 60 min of milling when the crystallite size was 21 nm, while the lattice distortion was 0.37%. Further milling had neither considerable influence on the crystallite size nor on the lattice distortion. Quantity of 14 mass% WC was introduced in the system during 60 min of milling. Specific surface area of the CeO_2 powders also increased with the milling time due to the particles fragmentation, but owing to the agglomeration of the particles the increase was slower after 30 min of milling

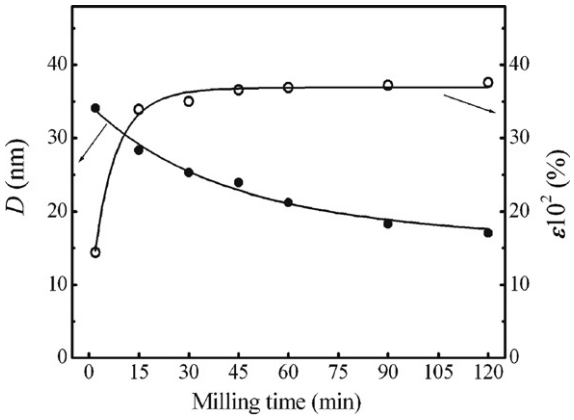

Fig. 2. CeO_2 crystallite size (D) and lattice distortion (ε) vs. milling time.

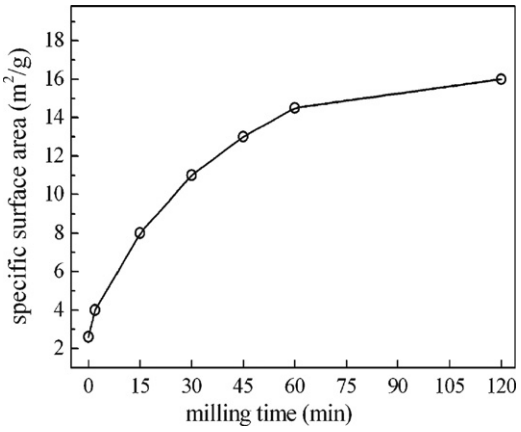

Fig. 3. Specific surface area of milled CeO_2 powders.

(Fig. 3). SEM microphotographs of the starting and 60 min milled CeO_2 powders (Fig. 4) confirm the existence of agglomerates in 60 min milled powder which are composed of the nanoparticles.

The nanocrystalline CeO_2 powder produced during 60 min of milling was selected for the investigation of the reduction. Also, with the aim of comparison, the starting CeO_2 powder was simultaneously thermally treated under the same reduction

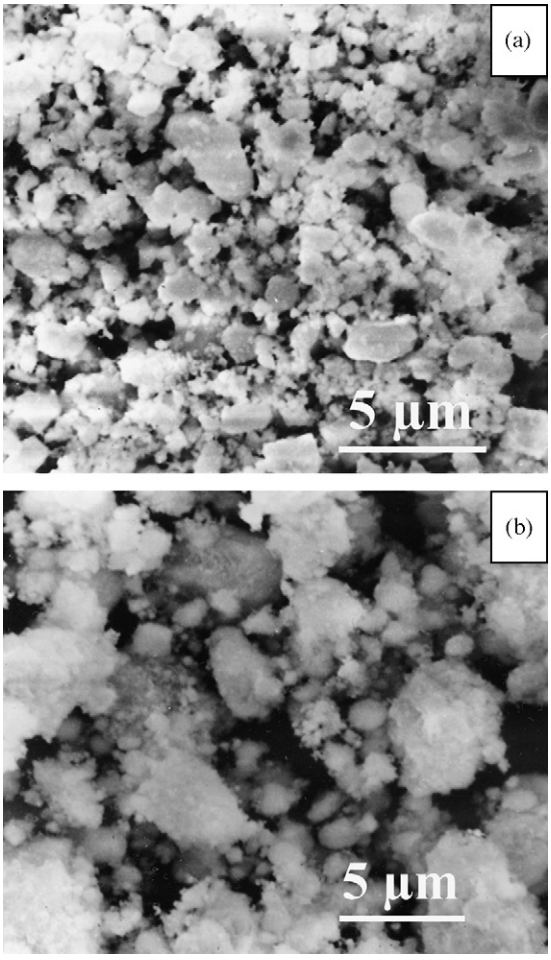

Fig. 4. SEM micrographs of (a) starting and (b) 60 min milled CeO_2 powders.

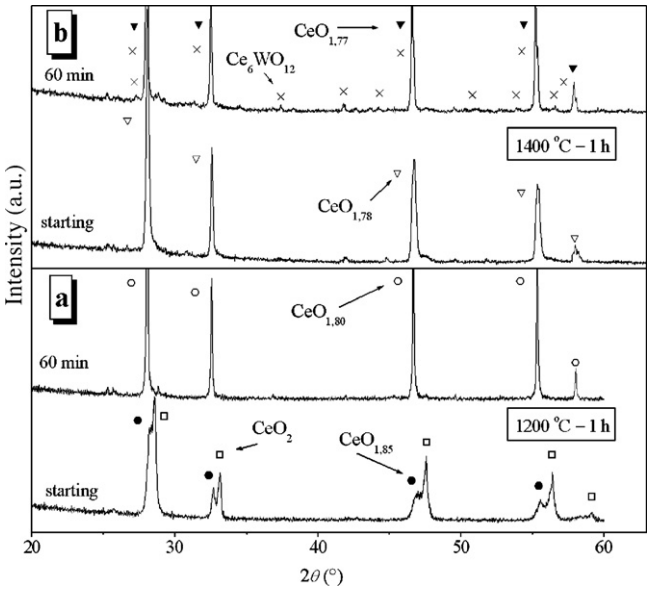

Fig. 5. Phases identified in starting and milled CeO_2 powders fired for 1 h at (a) 1200 °C and (b) 1400 °C.

conditions. During the thermal treatment in the temperature range 1200–1400 °C in an argon atmosphere, the nonstoichiometric CeO_{2-x} oxides with the fluorite structure were formed. XRD patterns of the both powders fired for 1 h at 1200 and 1400 °C are shown in Fig. 5, while in Table 1 the lattice parameter a and the composition of the identified CeO_{2-x} phases are summarized.

Nanocrystalline CeO_2 was completely reduced into nonstoichiometric oxide with composition $CeO_{1.80}$ during firing of 1 h at 1200 °C, while only 30 mass% of the starting CeO_2 powder was transformed into $CeO_{1.85}$ oxide. However, at 1400 °C for 1 h of firing both CeO_2 powders, starting as well as mechanically activated, were totally reduced into nonstoichiometric oxides both of which had similar composition, $CeO_{1.78}$ and $CeO_{1.77}$, respectively. Obviously, mechanical activation affects the rate as well as the level of the CeO_2 reduction. Since the $CeO_{1.80}$ composition obtained at 1200 °C from the activated powder is close to the composition $CeO_{1.78}$ obtained from the non-activated one at 1400 °C, it suggested that the reduction temperature of the nanocrystalline oxide is lowered for approximately 200 K after mechanical energy had been introduced into the system.

Reduction of CeO_2, as the gas–solid reaction, is mainly affected by the surface area contact of the solid phase, which is not only higher in mechanically activated powder but also has

Table 1
Lattice parameter a and composition of CeO_{2-x} oxides identified in fired CeO_2 powders

CeO_2	1200 °C–1 h		1400 °C–1 h	
	a (Å)	CeO_{2-x}	a (Å)	CeO_{2-x}
Starting	5.412(1)	CeO_2	–	–
	5.483(2)	$CeO_{1.85}$	5.512(1)	$CeO_{1.78}$
60 min milled	5.507(1)	$CeO_{1.80}$	5.518(1)	$CeO_{1.77}$

different crystal structure in comparison to the bulk of powder. Both parameters accelerate the oxygen release from the powder surface accompanied with the formation of oxygen vacancies as well as Ce^{3+}-ions for the charge neutrality preservation. In addition to that, almost the ten times smaller crystallite size and the high crystal lattice distortion in mechanically activated powder enhance diffusion of oxygen ions through the lattice. Also, the grate defect density in the grain boundary facilitates oxygen transport, resulting in higher reduction of nanocrystalline CeO_2 at 1200 °C. On the contrary, the slightly higher reduction of both CeO_2 powders at 1400 °C, which gives almost identical compositions ($CeO_{1.78}$ and $CeO_{1.77}$), is mainly caused by the rise of the rate of oxygen diffusion from inside the grains towards the grain boundaries due to temperature rise, which also influences the growth of crystallites and grains and the relax of crystal lattice distortion in mechanically activated powder.

WC present in the milled powder acts as a reducing agent producing Ce_2O_3 and WO_3, which react and give a small quantity of the Ce_6WO_{12} ($3Ce_2O_3{\cdot}WO_3$) compound, identified (PDF 23-1049) in the sample fired at 1400 °C. Identification was done according to the Ce_6WO_{12} superlattice reflections of the low intensities, since the main reflections of this compound are overlapped with the CeO_{2-x} reflections [17]. Superlattice reflections were not observed at 1200 °C due to the poor crystallization, compared to the one at 1400 °C.

4. Conclusions

The CeO_2 reduction in the microcrystalline and nanocrystalline powders in argon atmosphere at 1200 and 1400 °C was investigated. Starting CeO_2 powder, with the particles size less than 5 μm and the crystallite size of 140 nm, was milled for various times in a high energetic vibratory mill. During 60 min of milling, CeO_2 powder with the specific surface area of 14 $m^2\ g^{-1}$ was obtained. At the same time, the crystallite size of CeO_2 was reduced up to nanometer dimension of 21 nm, while the lattice distortion became 0.37%. Prolongation of milling had no considerable effect on the CeO_2 nanostructure. Milling did not affect the lattice parameter of CeO_2. Thermal treatment of CeO_2 powders, starting and 60 min milled, produced the nonstoichiometric CeO_{2-x} oxides with the fluorite structure. Composition of CeO_{2-x} oxides was calculated from their lattice parameter. At 1200 °C, the rate and the degree of the reduction of nanocrystalline CeO_2 was more efficient, providing entire reduction into $CeO_{1.80}$ oxide. On the contrary, the $CeO_{1.85}$ composition was obtained through the reduction of only 30 mass% of microcrystalline CeO_2. The reduction temperature of the nanocrystalline oxide is lowered for approximately 200 K. The higher specific surface area, lattice distortion and the reduced crystallite size of mechanically processed CeO_2 powder are the main parameters affecting gas–solid reaction of the CeO_2 reduction. The intensified reduction of both CeO_2 powders at 1400 °C is mainly caused by the rise of the oxygen rate diffusion.

Acknowledgment

The financial support of the Ministry of Science of Serbia is gratefully acknowledged.

References

[1] L. Kepinski, M. Wolcyrz, M. Marchewka, Structure evolution of nanocrystalline CeO_2 supported on silica: effect of temperature and atmosphere, J. Solid State Chem. 168 (1) (2002) 110–118.
[2] A. Trovarelli, M. Boaro, E. Rocchini, C. de Leitenburg, G. Dolcetti, Some recent developments in the characterization of ceria-based catalysts, J. Alloy Compd. 323–324 (2001) 584–591.
[3] T. Tago, S. Tashiro, Y. Hashimoto, K. Wakabayashi, M. Kishida, Synthesis and optical properties of SiO_2-coated CeO_2 nanoparticles, J. Nanoparticle Res. 5 (1-2) (2003) 55–60.
[4] M. Zinkevich, D. Djurovic, F. Aldinger, Thermodynamic modeling of the cerium–oxygen system, Solid State Ionics 177 (11–12) (2006) 989–1001.
[5] M. Mogensen, N.M. Sammes, G.A. Tompsett, Physical, chemical and electrochemical properties of pure and doped ceria, Solid State Ionics 129 (1–4) (2000) 63–94.
[6] S. Huang, L. Li, J. Vleugels, P. Wang, O. Van der Biest, Thermodynamic prediction of the nonstoichiometric phase $Zr_{1-z}Ce_zO_{2-x}$ in the ZrO_2–$CeO_{1.5}$–CeO_2 system, J. Eur. Ceram. Soc. 23 (1) (2003) 99–106.
[7] S. Huang, L. Li, O. Van der Biest, J. Vleugels, Influence of the oxygen partial pressure on the reduction of CeO_2 and CeO_2–ZrO_2 ceramics, Solid State Sci. 7 (5) (2005) 539–544.
[8] D. Terribile, A. Trovarelli, J. Llorca, C. de Leitenburg, G. Dolcetti, The synthesis and characterization of mesoporous high-surface area ceria prepared using a hybrid organic/inorganic route, J. Catal. 178 (1) (1998) 299–308.
[9] X. Yu, F. Li, X. Ye, X. Xin, Z. Xue, Synthesis of cerium(IV) oxide ultrafine particles by solid-state reactions, J. Am. Ceram. Soc. 83 (4) (2000) 964–966.
[10] T. Tsuzki, P.G. McCormik, Synthesis of ultrafine ceria powders by mechanochemical processing, J. Am. Ceram. Soc. 84 (7) (2001) 1453–1458.
[11] S.B. Bošković, B.Z. Matović, M.D. Vlajić, V.D. Krstić, Modified glycine nitrate procedure (MGNP) for the synthesis of SOFC nanopowders, Ceram. Int. 33 (1) (2007) 89–93.
[12] S. Bošković, D. Đurović, Z. Dohčević-Mitrović, Z. Popović, M. Zinkevich, F. Aldinger, Self propagating room temperature synthesis of nanopowders for SOFC, J. Power Sources 145 (2) (2005) 237–242.
[13] Joint Committee on Powder Diffraction Standards, International Centre for Diffraction Data, Powder Diffraction File, PCPDFWIN v.2.00, 1998.
[14] H.P. Klug, L.E. Alexander, X-ray Diffraction Procedures, John Wiley & Sons, New York, 1959.
[15] B. Lönnberg, Characterization of milled Si_3N_4 powder using X-ray peak broadening and surface area analysis, J. Mater. Sci. 29 (12) (1994) 3224–3230.
[16] D.J. Kim, Lattice parameters, ionic conductivities, and solubility limits in fluorite-structure MO_2 oxide ($M = Hf^{4+}$, Zr^{4+}, Ce^{4+}, Th^{4+}, U^{4+}) solid solutions, J. Am. Ceram. Soc. 72 (8) (1989) 1415–1421.
[17] M. Yoshimura, F. Sibieude, A. Rouanet, M. Foex, Identification of binary compounds in the system Ce_2O_3–WO_3, J. Solid State Chem. 16 (3–4) (1976) 219–232.